Low-frequency vibrations in a model glass

H. R. Schober and C. Oligschleger*
Institut für Festkörperforschung, Forschungszentrum Jülich, D-52425 Jülich, Germany
(Received 8 November 1995)

Previous simulation studies of localized low-frequency vibrational modes in a soft sphere glass are extended to larger samples. We find a boson peak in the spectral density and a maximum in the specific heat divided by T^3 similar to experiment. These maxima are caused by (quasi)localized vibrations. For finite frequencies these interact strongly with each other and with the extended phonons. This leads to an overdamping of the phonons around the boson peak and to a delocalization of the localized modes. A procedure to split the resulting modes into their bare constituents is presented. The bare localized modes are found to have a low-dimensional structure. The description in terms of the soft potential model is essentially verified.

I. INTRODUCTION

Glasses and amorphous materials in many respects resemble their ordered counterparts the crystals. The densities in both forms are normally similar. The elastic constants of the amorphous state are isotropic but otherwise of the same magnitude as in the crystal. Also the vibrational densities of state resemble each other. However, taking a closer look one finds a much richer dynamics in the disordered state, which is particularly obvious at low temperatures.[1,2] At low frequencies one observes the usual long-wavelength phonons (sound waves) in accordance with the elastic constants. At higher frequencies these phonons are strongly damped, and at some frequency, typically around 1 THz, the damping will exceed the Ioffe-Regel limit: The mean free path of the phonons diminishes below their wavelengths; the phonons are overdamped. This can be understood considering that whereas the long-wavelength phonons average over large regions of the glass the shorter-wavelength ones see the disorder on the scale of a few atomic distances. The vibrations can still be understood by harmonic theory but their eigenvectors will have a complicated structure reflecting the disorder.

Striking differences between the dynamics of glasses and amorphous materials are observed at low temperatures. The heat capacity is significantly larger than the value expected from the sound wave velocities. At temperatures below 1 K it increases linearly with T instead of $\propto T^3$ as given by the Debye model.[3] (In metallic solids there is an additional term $\propto T$ due to electronic excitations.) This anomaly in glasses has been explained by the standard tunneling model assuming a constant distribution of two-level tunneling states.[4,5] At somewhat higher temperatures the excess specific heat increases approximately $\propto T^5$. The frequency domain, corresponding to the excitations responsible, is accessible to spectroscopic methods like Raman[6] and neutron scattering.[7] From the temperature dependence of the measured intensities it has been deduced that the excitations are essentially harmonic vibrations which become increasingly anharmonic towards the lowest frequencies. These low-frequency vibrations coexist with the long-wavelength phonons and have been observed in a large variety of different glasses, e.g., metallic glasses,[8] vitreous silica,[7] and amorphous polymers.[9] Corresponding to the $c_p(T) \propto T^5$ variation of the specific heat the frequency spectrum of the excess vibrations increases as $Z(\nu) \propto \nu^4$ at low frequencies. The neutron scattering structure factor is consistent with excess vibrations localized to a few atoms[7] (''localized vibrations''). Due to their interaction with the extended sound waves, this localization cannot be exponential and the modes should more exactly be called resonant or quasilocalized.

At higher frequencies $Z(\nu)/\nu^2$ goes through a maximum ''boson peak.'' A corresponding maximum is observed in $c_p(T)/T^3$. Around the boson peak the extended phonons become overdamped and the distinction between localized and extended modes vanishes.

Additionally to these periodic excitations relaxations (aperiodic rearrangements) are observed in ultrasonic and dielectric relaxation experiments[10] already at low temperatures ($T > 5$ K). Depending on temperature and structure these can be envisaged as thermally activated incoherent tunneling or as hopping over some barrier. There will be a smooth transition from anharmonic vibrations to relaxations.

The above behavior can be described by the soft potential model (SPM), an extension of the standard tunneling model.[11,12] In this model it is assumed that one has in the glass some typical soft structure whose dynamics can be described by soft potentials. Due to the randomness of their local environment in the glass, the parameters of the potentials will be distributed according to some probability law. The resulting potentials can be single or double wells. The first describe soft vibrations whereas the latter ones, depending on barrier height, give additional tunneling states and relaxations. By fitting this model to the experimental data, one finds effective masses of 20–100 atomic masses for the entities moving in these effective soft potentials.[13,14]

The general behavior predicted by the SPM was confirmed by a computer simulation of a soft sphere glass (SSG) where quasilocalized modes with effective masses ranging from ten atomic masses upwards were found, Refs. 15,16, later referred to as I. The modes were centered at structural irregularities with large local strains. Regions of local strain have also been observed in earlier computer simulations.[17] Similar effective masses have since been observed in simulations of SiO_2,[18] Se (Ref. 19) in Ni-Zr[20] and Pd-Si,[21] in amorphous ice,[22] and in amorphous and quasicrystalline Al-Zn-Mg.[23] In an earlier simulation of amorphous silicon

low-frequency localized vibrations have been observed at coordination defects.[24]

In the soft potential model the local relaxations are strongly correlated with the local soft vibrations. Experimentally this is supported by the similarity of the structure factors of both types of excitations.[7] At temperatures above a few kelvin these local relaxations can be envisaged as a change of configuration by thermally activated hopping of some group of atoms over a barrier. From diffusion measurements in a metallic glass again effective masses of 10 have been derived for this collective motion.[25] Strong correlations between soft vibrations and hopping have been observed in molecular dynamics simulation of the SSG (Ref. 26) and in amorphous Se.[27] Both reversible and irreversible relaxations were observed which consist of a collective hopping of groups of atoms. Collective hopping motions have been also observed in simulations of binary Lennard-Jones and soft-sphere mixtures above and below the glass-transition temperature[28,29] and in amorphous Ar after introduction of vacancies.[30] Heuer and Silbey[31] systematically searched for double-well potentials in a binary model glass at $T=0$. They found a distribution of two well potentials in qualitative agreement with the soft potential model. The effective masses of the jump modes from one well into the other ranged from two atomic masses upward. This low number might be affected by the static search algorithm where the nearest neighbor shell of an atom is first displaced and then allowed to relax. By this procedure and due to the small system size, more extended collective motions over lower barriers might be broken up, particularly for the larger jump distances. Bembenek and Laird[32] used the instantaneous mode technique[33] to study double-well potentials in the SSG. They find them to be connected with jumps of small numbers of atoms at low temperatures. With increasing temperatures they observe a delocalization in the temperature region of the glass transition.

In the present paper we extend our earlier investigations on the soft sphere glass, I, to larger systems. This enables us to study in detail the effects of interactions of the local vibrational modes with each other and with extended phonons. In the following section we give details of the computational procedure. The vibrational modes are calculated and properties connected with their spectra discussed. Analyzing their eigenvectors we find at low frequencies besides quasilocalized and extended phononlike modes a large number of modes resulting from the interaction of these. At low frequencies this mixture of modes can be disentangled and one thus gains ''pure'' extended and localized modes whose properties can be studied. These modes are used to validate the assumptions of the soft potential model.

II. COMPUTATIONAL DETAILS

The soft sphere glass (SSG) is described by an inverse sixth-power potential

$$u(r)=\epsilon\left(\frac{\sigma}{r}\right)^6+A\left(\frac{r}{\sigma}\right)^4+B. \tag{1}$$

To simplify the computer simulation and normal-mode analysis, the potential is cut off at $r/\sigma=3.0$, and then shifted by a polynomial $A(r/\sigma)^4+B$, where $A=2.54\times10^{-5}\epsilon$ and $B=-3.43\times10^{-3}\epsilon$ were chosen so that the potential and the force are zero at the cutoff. This form of the shifting function was chosen so that its effect is negligible near $r/\sigma=1.0$. Quantities such as the pressure and average potential energy will be changed by a few percent as a result of this truncation, but any changes in the equilibrium structure will be small. At any rate, our interest is in the existence and characterization of low-frequency localized vibrational modes in general, and not in a quantitative description for any specific potential. Without loss of generality one can set $\epsilon=\sigma=m=1$. Where we do not explicitly state the units we infer these ''system units.''

The inverse sixth-power potential was selected because it is a well-studied theoretical model that qualitatively mimics many of the structural and thermodynamic properties of bcc-forming metals including the existence, in its bcc crystal form, of very soft shear modes,[34] and it was hoped that this property would be reflected in a high concentration of low-frequency resonant modes in the glass. As evidence of the universality of the phenomena discussed here, we also found low-frequency resonant modes in one- and two-component Lennard-Jones systems, but at such a low concentration that the collection of any reasonable statistics would have been very difficult.

An estimation of the glass-transition temperature was obtained in I by calculating the diffusion constant D of the system at this density as a function of the reduced temperature using the relation

$$D=\lim_{t\to\infty}\frac{1}{6t}\langle|\vec{R}(0)-\vec{R}(t)|^2\rangle, \tag{2}$$

where $\vec{R}(t)$ is the time-dependent position vector of a particle and $\langle\cdots\rangle$ denotes a configurational average. The diffusion constant so calculated is very well fit by a fractional power law

$$D=A(T-T_0)^{\alpha}, \tag{3}$$

with $A=0.191$, $\alpha=1.21$, and $T_0=0.085$. That such a fitting function so well describes the diffusion data is consistent with the predictions of mode-coupling theory.[35] The temperature T_0 can be taken as a lower limit for the glass-transition temperature, since below T_0 diffusive motion is effectively frozen out.

We extended our previous study of configurations of 500 and 1024 atoms to larger systems by quenching well-equilibrated liquid configurations of 5488 soft spheres produced via constant-energy molecular dynamics (MD) simulation with cubic periodic boundary conditions again at a density $\rho\sigma^3=1.0$ and temperature $kT/\epsilon\approx0.54$ (about 2.5 times the melting temperature at this density[36]). For the simulation, we used the velocity-Verlet algorithm[37] with a time step of 0.04, in units of $(m\sigma^2/\epsilon)^{1/2}$. The liquid is first quenched within the MD simulation by velocity rescaling to a reduced temperature of about $0.005T_g$. The quench rate was about $0.015k/(m\sigma^2\epsilon)^{1/2}$. After the MD quench, each sample was heated to $0.05T_g$ and aged for several 1000 further MD time steps to stabilize the potential energy and to avoid spurious minima. Each system is then quenched to zero temperature using a combination steepest-descent–

conjugate-gradient algorithm.[38] The resulting potential energy equals roughly the one of the fcc crystals of the same density with about 1.5% Frenkel defects. Together with the previous work, in all, 60, 21, and 15 different configurations of 500, 1024, and 5488 atoms, respectively, were created in this way and analyzed.

To illustrate the glassy nature of our zero-temperature sample and to aid comparison of this model glass to real materials the configurationally averaged structure factor $S(k)$ for our system has been shown in I.

To study the glasses at elevated temperatures the quenched glasses were heated in stages to 5%, 10%, and 15% of the glass temperature. At each temperature the glasses were observed for 90 000 time steps, corresponding to about 5000 vibrations of an average frequency. Some results on the relaxations have been published elsewhere.[27] In the present investigation the resulting configurations are only used to check for effects of annealing.

III. SPECTRA AND LOCALIZATION OF VIBRATIONAL MODES

The harmonic vibrations of each glass configuration were calculated from the force constant matrix of the $T=0$ minimum configuration. The numerically exact minimization of the potential energy prevents the occurrence of spurious unstable modes. The elements of the force constant matrix are given by

$$D_{\alpha\beta}^{mn}=\frac{\partial^2 u(|\mathbf{R}^m-\mathbf{R}^n|)}{\partial R_\alpha^m \partial R_\beta^n}. \tag{4}$$

Whereas for the two sets of smaller configuration a direct diagonalization was possible, computer storage limitations make this impossible for the large configurations ($N=5488$). For these only the lowest vibration modes ($\nu<0.2$) were calculated by sparse matrix techniques.[39] The frequency spectra are calculated from the frequencies of the $3N-3$ vibrational modes σ as

$$Z(\nu)=\left\langle \frac{1}{3N-3}\sum_\sigma \delta(\nu-\nu^\sigma)\right\rangle, \tag{5}$$

where δ is the discretized δ function and $\langle\cdots\rangle$ stands for the averaging over configurations. The calculated spectra for the small and large configurations fit smoothly at $\nu=0.2$. We therefore used for the higher ν values the spectra calculated for $N=500$.

For comparison we calculated the Debye spectrum

$$Z_{\text{Debye}}=\frac{3}{\nu_D^3}\nu^2, \tag{6}$$

with

$$\nu_D=\bar{c}\left(\frac{3\rho}{4\pi m}\right)^{1/3} \tag{7}$$

and the average sound velocity $\bar{c}$ given in terms of the longitudinal and transverse velocities c_ℓ and c_t. These are calculated from the elastic constants of the glass by the usual relation $c_\ell=\sqrt{c_{11}/\rho}$ and $c_t=\sqrt{c_{44}/\rho}$ where we employ the elastic isotropy of the glass.

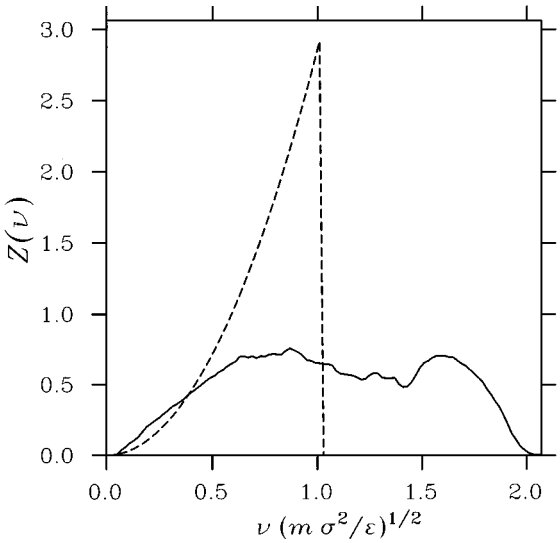

FIG. 1. Configurationally averaged vibrational density of states of the soft sphere glass (solid line) and Debye spectrum (dashed line).

We calculated the elastic constants from the change in potential energy, ΔE, under an applied strain

$$R_\alpha^m \to R_\alpha^m+\sum_\beta \epsilon_{\alpha\beta}R_\beta^m, \tag{8}$$

$$\Delta E=-\sum_{\alpha\beta} P_{\alpha\beta}\epsilon_{\alpha\beta}+\frac{V}{2}\sum_{\alpha\beta\gamma\delta}\epsilon_{\alpha\beta}C_{\alpha\beta\gamma\delta}\epsilon_{\gamma\delta} + \frac{1}{2}\sum_{\alpha\beta\gamma} P_{\alpha\beta}\epsilon_{\alpha\gamma}\epsilon_{\gamma\beta}. \tag{9}$$

Here the first term accounts for the work done against the forces for an ensemble which is not in equilibrium against volume changes, as is the case for the purely repulsive potential considered here. $P_{\alpha\beta}$ is the virial of the forces. The third term, present for shears only, is a correction for the volume change under a finite shear in such a lattice and the $C_{\alpha\beta\gamma\delta}$ are the elastic constants ($c_{11}=C_{1111}, c_{44}=C_{2323}$).

We find for the glass the sound velocities $c_\ell=4.96$ and $c_t=1.45$ in units of $\sqrt{\epsilon/m}$. Taking the finite size of the ensemble this implies that the lowest-frequency phonon which could be observed for the largest samples is at $\nu=0.082$. The elastic anisotropy of a single configuration is found to be less than 1%.

Figure 1 shows the vibrational density of states averaged over all configurations together with the Debye spectrum. One sees a clear enhancement of the glassy spectrum at low frequencies which reaches well beyond frequencies where system sizes could be of importance. The small indentation of the spectrum around $\nu=1.4$ is a property of the $1/r^6$ potential. It disappears for higher-power (harder) potentials ($1/r^n$ with $n\approx 9$).

From the density of states we can calculate the vibrational specific heat at constant volume. In harmonic approximation one has per atom

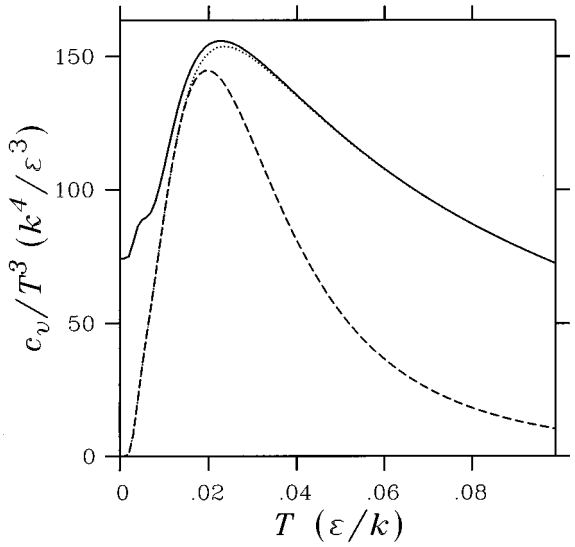

FIG. 2. Specific heat divided by T^3 plotted against temperature (dotted line, values derived from the spectrum of Fig. 1; dashed line, contributions of modes with $\nu<0.18$ only; solid line, full spectrum with Debye correction).

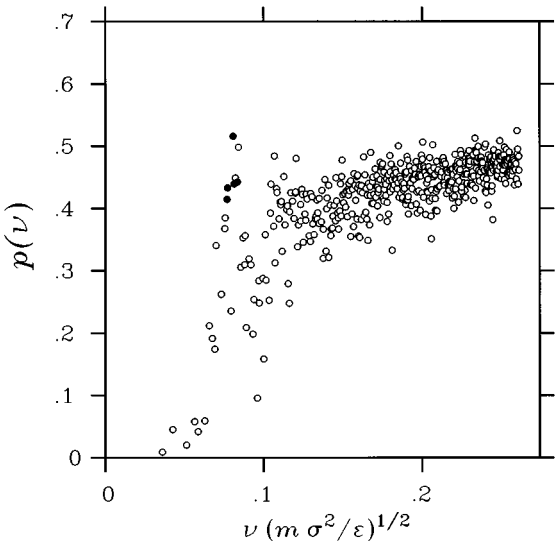

FIG. 3. Participation ratios of low-frequency modes of one soft sphere glass configuration with $N=5488$ atoms plotted against frequency. Solid circles depict those modes whose overlap with the idealized phonons of longest permitted wavelength exceeds 0.5.

$$c_v=3k\int d\omega\left[\left(\frac{\hbar\omega}{2kT}\right)^2\Big/\sinh^2(\hbar\omega/2kT)\right]Z(\omega). \quad (10)$$

The vibrational specific heat of a perfect crystal is at low temperatures $\propto T^3$. It is, therefore, usual practice to plot c_v/T^3. In such a plot a Debye spectrum gives a constant whereas in glasses an increase above this constant is found. Figure 2 shows this behavior for the soft sphere glass. The dotted line shows the values gained from the spectrum of Fig. 1 and the dashed line the contribution of the low-frequency modes only ($\nu<0.18$). To correct for the finite size of the simulated glass we added to the spectrum a Debye contribution up to a frequency below the one of the lowest possible phonon frequency. This correction amounts to a fraction of 3×10^{-4} of all modes. The resulting values for the specific heat are shown by the solid line. No effort was made to smooth the discontinuity due to this correction. The plot shows a maximum of about twice the Debye value just above a temperature of 0.02 in reduced units. This is comparable to the usual values in glasses. This maximum is caused by the excess low-frequency modes.

Diagonalization of the force constant matrix, Eq. (4), gives besides the eigenvalues also the eigenvectors. These give the structure of the vibration and can, e.g., be used to determine the localization of the vibration. There are two usual measures of localization, namely, the effective mass and the participation ratio which both have been calculated in our previous work. The effective mass is given in terms of the eigenvector as

$$m_{\rm eff}(\sigma)=m/|\mathbf{e}^1(\sigma)|^2. \quad (11)$$

Here we have assumed that the $3N$-dimensional unit vector of mode σ is normalized and $\mathbf{e}^n(\sigma)$ stands for the vector formed from the three components on atom n. Atom No. 1 is taken as the atom with the largest displacement. $m_{\rm eff}/m$ is a measure for the number of atoms which effectively carry the kinetic energy of the vibrational mode. This definition is limited to small system sizes when the long-range tails of the modes are not too important. In the following we will use mainly the participation ratio

$$p(\sigma)=\left(N\sum_{n=1}^{N}|\mathbf{e}^n(\sigma)|^4\right)^{-1}. \quad (12)$$

For a translation one has $p=1$ and for a vibration of a single atom with all others at rest $p=1/N$. This scaling with $1/N$ should hold for all localized modes. Figure 3 shows the participation ratios of the lowest-frequency modes for one configuration of $N=5488$ atoms. The lowest-frequency modes are as expected highly localized. Their participation ratio shows compared to the most localized modes of the $N=500$ and $N=1024$ configurations the expected $1/N$ scaling. It corresponds to a localization to about 20 atoms in terms of the effective mass. At a frequency of around $\nu=0.08$ one observes a slight maximum in p. This corresponds to extended modes, the lowest-lying phonons permitted by the system size [transverse $(q,0,0)$ phonons]. We find 5 modes whose overlap factors with the 12 idealized phonons exceed one-half. Between the maximally and minimally localized modes a large number of modes with intermediate participation ratios is found. As we will see below these modes are formed by interactions of localized modes and phonons. Above $\nu=0.1$ the second group of phonons can be observed. At higher frequencies a broad band of participation ratios is formed which slowly rises to an average value of about 0.6 as shown earlier for the smaller systems.

There is a number of effects which contribute to this spread of participation ratios, all connected with interaction between ''pure'' vibrational modes. First the participation ratio of degenerate modes is not well defined. Let us take the group of lowest transverse phonons in our simulation. Their wave vectors are $\mathbf{q}=(q_{\rm min},0,0)$ where $q_{\rm min}=2\pi/L$ with L the periodicity length. There are 12 phonons of this type,

given, e.g., by sin and cos in the three spatial directions and the two transverse polarizations. If these 12 modes are degenerate, any superposition of these modes is again an eigenmode. By suitably superimposing the six phonons one can so vary the participation ratio p between 0.44 and 1. E.g., a superposition $(1,0,0)\cos(q_{\min}R_x)+(0,1,0)\sin(q_{\min}R_y)$ gives $p=1$. In a disordered medium the degeneracy is lifted by scattering at disorder and on ''extra vibrational modes.'' The resulting phonon eigenvectors will have participation ratios in the above range, always assuming that the scattering is not too strong.

In amorphous materials and glasses one finds at low frequencies besides the phonons additional modes. For the soft sphere glass this is evident from Fig. 1. In I we have shown that these modes are localized, although not in the strict sense of this term. It is well known from lattice dynamics, e.g. Ref. 40, that the interaction between local vibrations and phonons prevents true localization of harmonic vibrations with frequencies inside the band of phonon frequencies. The local vibration will be dressed by a cloud of phonons and becomes a quasilocalized or resonant vibrational mode. The phonons will be broadened (damped) by the scattering at the defects. In crystals it has been shown that the interaction between defect vibrations and host phonons can be so strong as to destroy the phononic character already for defect (''local vibration'') concentrations of order 10^{-3}.[41]

If we take the low-frequency behavior of the glass as constituted from extended phonons and local vibrations, this has the following consequences. The phonons will be broadened in addition to the scattering at the static disorder by their interaction with the local vibrations. The admixture of the local vibrations will tend to reduce their participation ratio. Since the concentration of local vibrations increases with frequency, the phonons will eventually lose their character. The local vibrations on the other hand will delocalize and their participation ratio will tend to increase. The delocalization in turn causes local vibrations of similar energy to interact. Depending on the strength of interaction, the two combined modes will have participation ratios somewhere between the single ones and their sum. For a finite concentration, c, of interacting modes the scaling factor $1/N$ in Eq. (11) will be replaced by c.

We have used the above picture to approximately disentangle the exact low-frequency modes into their constituents: local vibrations and extended phonons. We assume that the constituent (unmixed) modes $\mathbf{e}'$ modes can interact with all modes of frequencies of $\pm 20\%$. The resulting eigenmodes $\mathbf{e}$ will be linear combinations of the extended or localized ''unmixed'' modes,

$$\mathbf{e}(\nu)=\sum_{0.8\nu<\nu'<1.2\nu} a(\nu,\nu')\mathbf{e}'(\nu'), \tag{13}$$

where we labeled the modes by their frequencies and the $a(\nu,\nu')$ are the expansion coefficients. To invert Eq. (13) approximately, we use that the $\mathbf{e}'$ modes are either localized, with a small participation ratio, or extended, with participation ratios $p>0.4$. We restrict ourselves to low frequencies where the density of localized modes is low and we can neglect the overlap between the unmixed localized modes $\mathbf{e}'$. Since the mixing of the modes will increase the participation ratios p of these modes, we can use a minimum condition in p to extract the modes from the exact (mixed) modes $\mathbf{e}$. We start with the most localized mode, eigenvector $\mathbf{e}(\nu_1)$, and cycle over all modes it can interact with and which have a higher participation ratio. We rotate the basis of eigenvectors in pairs $(\nu_1\nu_2)$ such that the participation ratio of the rotated mode is minimal,

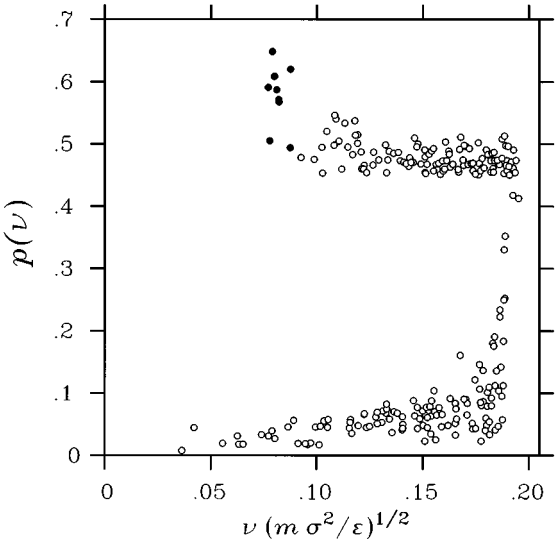

FIG. 4. Participation ratios of low-frequency modes after demixing for the soft sphere glass configuration of Fig. 3. Solid circles depict those modes whose overlap with the idealized phonons of longest permitted wavelength exceeds 0.5.

$$\mathbf{e}'(\nu_1')=R_{11}\mathbf{e}(\nu_1)+R_{12}\mathbf{e}(\nu_2),$$

$$\mathbf{e}'(\nu_2')=R_{12}\mathbf{e}(\nu_1)+R_{22}\mathbf{e}(\nu_2). \tag{14}$$

The new frequencies ν' are defined by the expectation value of the dynamical matrix (4) with the new eigenvectors $\mathbf{e}'$. These rotations are done for all pairs of modes, less than 20% apart in frequency, until all modes with $p<0.4$ have been dealt with. This limit has been chosen to prevent extended phonons from being forced to localize. The above procedure ensures the separation of phonon tails from the local modes and the breakup of interacting local modes into their constituents.

At any stage the modes $\mathbf{e}'$ form a complete orthogonal basis. To avoid an artificial breakup of modes we apply this method only to the lowest 1% of all modes. The low density of states in this region together with the $\nu\pm 20\%$ cutoff in the allowed interaction causes then each mode to interact only with a small number of neighboring modes. This would no longer be the case for modes in the middle of the spectrum. For the low-frequency tail of the spectrum we expect our method to give a fairly good representation of the underlying modes. Of course the orthogonality condition will burn small holes into the extended modes. Due to the small mode densities, these will have negligible effect. In Fig. 4 we show the resulting participation ratios after having processed the modes used for Fig. 3. Comparing the two figures one sees that the modes have been divided into localized ones $(p<0.1)$ and extended ones $(p>0.4)$. The rapid increase of

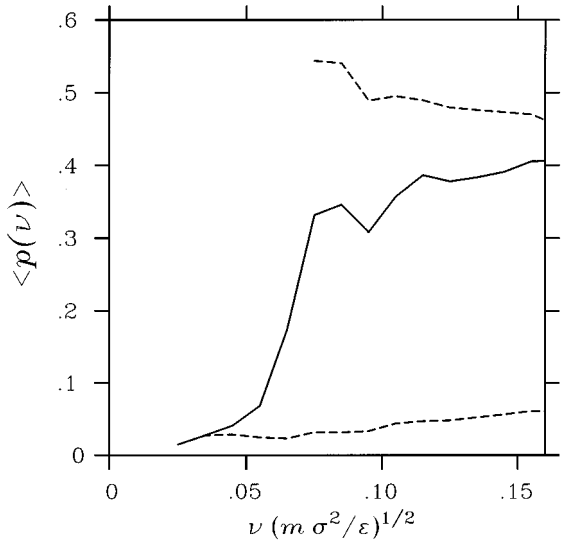

FIG. 5. Ensemble-averaged participation ratios for the soft sphere glass with $N=5488$ atoms plotted against frequency (solid line, original modes, dashed lines, localized and extended modes after demixing).

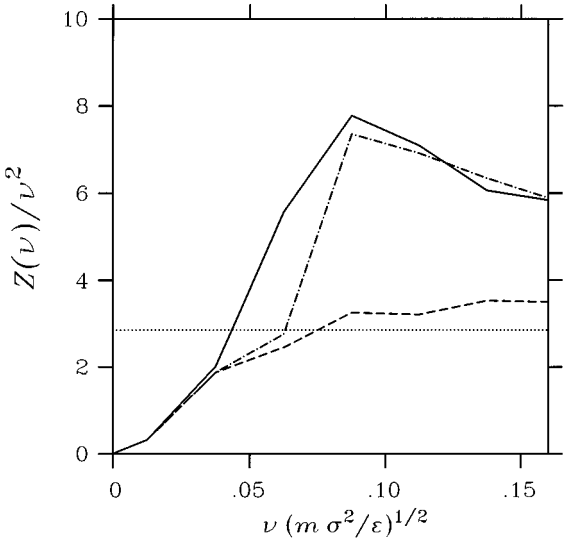

FIG. 6. Low-frequency part of the spectrum divided by ν^2 (solid line, spectrum of Fig. 1; dash-dotted line, spectrum after demixing; dashed line, spectrum of local modes after demixing; dotted line, Debye spectrum).

p near $\nu=0.2$ is an artifact of the cutoff of the modes used in the procedure, Eq. (13). Only the modes up to $\nu=0.15$ have been treated properly. The lowest two groups of extended modes (phonons) can be discerned. There are ten modes whose overlap factor with the idealized transverse $(q,0,0)$ phonons of maximal wavelength exceeds 0.5. Ideally one should have 12 such modes. The deficiency can be attributed to the overlap between the phonons; see below. Comparing the frequencies of the modes in Figs. 3 and 4 we find small shifts of a few percent between the two sets of modes.

The ensemble averages of the participation ratios of the localized and extended modes are shown in Fig. 5. The solid line depicts the overall average of the participation ratios of the original modes. The minimum around $\nu=0.9$ corresponds to the gap between the two lowest phonons which is an effect of the finite size. Above $\nu=0.1$ the values increase slowly toward $p\approx 0.55$ which is reached outside the range of this plot. The dashed lines depict the participation ratios of the localized and extended modes, respectively, which were obtained by the decoupling procedure. There is a slight increase with frequency of p of the localized modes accompanied with a decrease for the extended ones. This might be due to an incomplete demixing of the modes. The average effective mass, Eq. (11), is around 20 in units of m and increases slightly to 40 for $\nu=0.16$. As for the corresponding increase in p, it is not clear how much of this increase is an artifact of an incomplete decoupling. The numbers agree with the ones previously published for the $N=500$ and $N=1024$ systems. Particularly encouraging is the agreement in the frequency range where there are extended modes in the large system and none in the small system. We can exclude size effects and major effects due to the demixing.

To show the contributions of the distribution of the different modes we plot in Fig. 6 the spectrum divided by ν^2. In such a representation the Debye spectrum is a constant (dotted line). The spectrum of the original modes is given by the solid line, the one of the modes after demixing by the dash-dotted line, and the one of the localized modes by the dashed line. There is only a slight change of the spectrum due to the demixing. The part of the spectrum shown contains about 8×10^{-3} of all modes. About 4% of the original modes in this frequency range have been shifted by the demixing to frequencies above the shown limit of $\nu=0.16$. Around $\nu=0.08$ there is a maximum in $Z(\nu)/\nu^2$, the so-called boson peak. The excess over the Debye contribution is about 1.5 of the latter. We cannot locate the boson peak exactly due to statistics. Furthermore, for the given system size it lies very close to the first group of extended modes. To avoid the problems in the spectrum of extended modes due to system size, one can define a spectrum of noninteracting modes by adding the Debye and the local mode spectra. The boson peak for this spectrum would be at $\nu\approx 0.15$. This means that by softening some localized modes the interaction between modes shifts the boson peak to lower frequencies.

The increase in the localized mode density of states at low frequencies is at least $\propto\nu^3$ and is compatible with the $Z_{\rm loc}\propto\nu^4$ behavior predicted by the soft potential model.[13] We will discuss our results concerning this model below.

IV. STRUCTURE OF VIBRATIONAL MODES

To get insight into the structure of the extended modes as they would be seen by neutron Brillouin scattering we define a structure factor for a given $\mathbf{q}$ as

$$S(\mathbf{q},\nu)=\sum_{\sigma}\left[\sum_{m,n}^{N} e^{i\mathbf{q}(\mathbf{R}^n-\mathbf{R}^m)}(\mathbf{e}^m(\sigma)\cdot\mathbf{e}^n(\sigma))\right]\delta(\nu-\nu^\sigma). \tag{15}$$

In a real glass all $\mathbf{q}$ directions are equivalent, one observes an angular average. For our finite size simulation we have to replace this average by a sum over all $\mathbf{q}$ vectors of length q, allowed by periodicity,

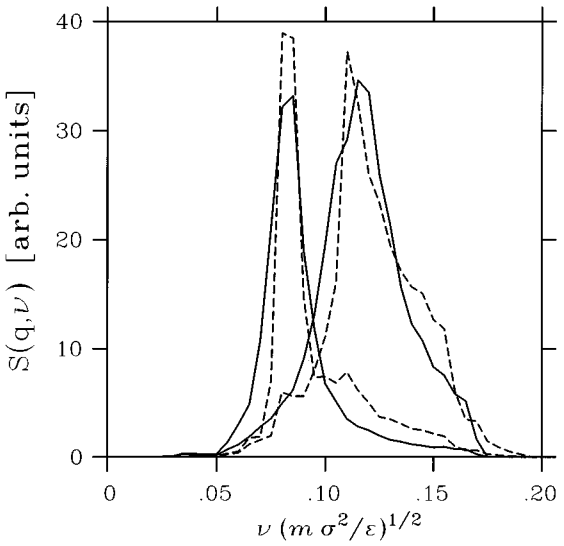

FIG. 7. Structure factor for the two lowest-frequency phonon groups $\mathbf{q}=(q_{\min},0,0)$ and $\mathbf{q}=(q_{\min},q_{\min},0)$ as function of frequency (solid line, original modes; dashed line, modes after demixing). The phonon frequencies calculated from the sound velocity are $\nu=0.082$ and $\nu=0.116$, respectively.

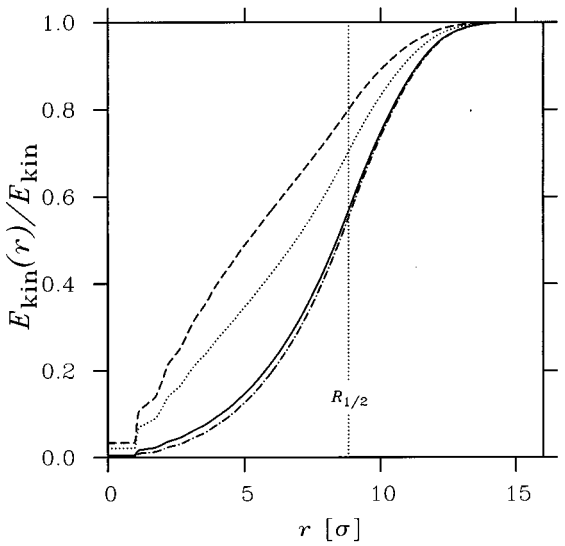

FIG. 8. Fraction of the kinetic energy of the low-frequency vibrational modes contained in a sphere of radius r (solid line, average over all original modes; dash-dotted line, average over extended modes after demixing; dashed line, average over localized modes after demixing; dotted line, average over all modes after demixing). $R_{1/2}$ denotes half the periodicity length.

$$S(q,\nu)=\sum_{|\mathbf{q}|=q} S(\mathbf{q},\nu). \tag{16}$$

In Fig. 7 we show $S(q,\nu)$ for the two lowest q values allowed, corresponding to phonons with the wave vectors $\mathbf{q}=(q_{\min},0,0)$ and $\mathbf{q}=(q_{\min},q_{\min},0)$, respectively.

The solid and dashed lines show the structure factors for the original and modified modes, respectively. $S(q,\nu)$ peaks at the frequencies of the transverse phonons as calculated from the elastic constants ($\nu=0.082$ and $\nu=0.116$). The corresponding longitudinal frequencies are outside the frequency range of the figure. The demixing does not shift the peak positions significantly. The apparent shift of the second peak is caused by the finite size of the chosen frequency bins and the shoulders on the high-frequency side. These are an artifact of the procedure. In those frequency ranges where different phonon groups overlap the long-range tails of the localized modes can get attached to the ''wrong'' extended modes, thus feigning an increased interaction of the extended modes. No effort was taken to reduce these shoulders.

Taking an approximate Lorentzian line shape

$$S(q,\nu)=\frac{\Delta\nu}{\pi}\,\frac{1}{(\nu-\nu_0)^2+(\Delta\nu/2)^2}, \tag{17}$$

we find $\Delta\nu=0.018$ for the first phonon and 0.036 for the second one. The widths are strongly reduced by the demixing to $\Delta\nu=0.012$ and $\Delta\nu\approx0.025$. The last value was taken from the low-frequency side only.

The width $\Delta\nu$ is caused by two effects, the scattering on the static disorder and the scattering between soft modes and extended phonons. If we assume complete demixing, the dashed lines show the broadening due to the static disorder only. Both effects contribute equally to $(\Delta\nu)^2$. The total width $\Delta\nu$ increases $\propto\nu^2$, i.e., $\propto q^2$. Since in the frequency range of the two phonon groups considered the density of local modes is nearly constant, this means an increase of the coupling to the local modes $\propto q^2$. This q dependence of the phonon damping is observed in crystals for resonant scattering by resonant vibrations of even symmetry. An example is the self-interstitial in Cu or Al where one atom is replaced by a pair of atoms (dumbbell configuration) and where the transverse phonons are strongly damped by the librations of these dumbbells.[41]

It has been argued before[42] that at the boson peak the Ioffe-Regel limit is reached for the phonons; i.e., their mean free path decreases to their wavelength ($2\pi\Delta\nu/2\approx\nu$). This limit is reached for our first phonon group which approximately coincides with the boson peak; see Fig. 6. In the absence of scattering between soft modes and extended phonons the Ioffe-Regel limit would be reached only for higher frequencies.

A measure for the spatial extent of the modes is the degree of localization of the kinetic energy. Defining the central atom (atom 1) as the atom that has for a given mode the largest amplitude we can calculate the fraction of the kinetic energy residing within a sphere of radius r around this central atom as

$$\frac{E^{\sigma}_{\mathrm{kin}}(r)}{E^{\sigma}_{\mathrm{kin}}}=\sum_{|\mathbf{R}^m-\mathbf{R}^1|<r}\left|\mathbf{e}^m(\sigma)\right|. \tag{18}$$

The $r=0$ value in such a plot is m/m_{eff} of Eq. (11). For an extended mode, $\propto\cos(\mathbf{q}\cdot\mathbf{R})$, $E^{\sigma}_{\mathrm{kin}}(r)$ should increase as r^2. This behavior is shown in Fig. 8 for both the average of all modes up to $\nu=0.16$ (solid line) and the extended modes after demixing (dash-dotted line).

In I the same behavior was reported for the average over all modes. The energy distribution does not distinguish between the pure extended modes and the mixture of extended and localized modes. The periodicity length of the simulation

was 17.6, whence the radius of the inscribed sphere is $R_{1/2}=8.82$. The fraction of kinetic energy inside this sphere is about 0.56, compared to $\pi/6\approx 0.52$ for a constant amplitude. Contrary to this the ''noninteracting'' localized modes (dashed line) show a steeper than linear increase compatible with one-dimensional structures with amplitudes falling off with distance from the center. About 83% of the kinetic energy lies within the inscribed sphere and it takes a sphere with $r=4.4$ to include half of the kinetic energy. The latter implies chain lengths of eight nearest neighbor distances. As to be expected the average over localized and extended noninteracting modes (dotted line) lies in between. It shows the strong dependence of $E_{\rm kin}(r)$ on the base used to describe the vibrational modes.

The large contributions to $E_{\rm kin}$ from long distances make an assignment of dimensionality to the modes difficult. We define a tensor

$$G_{\alpha\beta}(\sigma)=\frac{\Sigma_n|\mathbf{e}^n(\sigma)|^\mu(R^n_\alpha-R^{\rm c.m.}_\alpha)(R^n_\beta-R^{\rm c.m.}_\beta)}{\Sigma_n|\mathbf{e}^n(\sigma)|^\mu}, \quad (19)$$

where we take the exponents $\mu=2$ and $\mu=4$, corresponding to the effective mass and participation ratio, respectively. $\mathbf{R}^{\rm c.m.}$ is the corresponding center-of-mass coordinate of the mode:

$$\mathbf{R}^{\rm c.m.}=\frac{\Sigma_n|\mathbf{e}^n(\sigma)|^\mu\mathbf{R}^n}{\Sigma_n|\mathbf{e}^n(\sigma)|^\mu}. \quad (20)$$

Diagonalizing G we obtain three eigenvalues $\rho^i(\sigma,\mu)$ and from these an average gyration radius[18,43]

$$R_{\rm gyr}(\sigma,\mu)=\sqrt{\frac{1}{3}\sum_i \rho^i(\sigma,\mu)}. \quad (21)$$

If a mode is localized on a single atom, $R_{\rm gyr}=0$, and for an extended mode it is the root-mean-square distance with the weight determined by μ. An effective dimension of the mode can be defined as

$$d(\sigma,\mu)=\sum_i \rho^i(\sigma,\mu) \Big/ \max\rho^i(\sigma,\mu). \quad (22)$$

Averaging over all modes with $\nu<0.16$ we get for the effective mass $\overline{R_{\rm gyr}}(2)=4.8$ and $\overline{d}(2)=2.5$ and slightly smaller values for the participation ratio $\overline{R_{\rm gyr}}(4)=4.4$ and $\overline{d}(4)=2.3$. These values imply that the modes extend over the whole simulation volume in accordance with Fig. 8. This in turn renders the so-defined dimension meaningless since the periodic boundary conditions fold the modes back into the periodicity volume. The values for the participation ratio are always smaller than the effective mass values due to the stronger weight on the central atoms. After the demixing of the modes we find the same values for the extended modes. For the localized modes we find smaller values $\overline{R_{\rm gyr}}(2)=3.6$, $\overline{d}(2)=2.6$ and $\overline{R_{\rm gyr}}(4)=1.3$, $\overline{d}(4)=2.0$. Due to the weighting with R^2, these values are strongly influenced by the long-range tails of the modes. To get an estimate of the effects of these tails we recalculated the values for the core of the modes, only including the atoms with $|\mathbf{e}^n|^2>0.2\max|\mathbf{e}^n|^2$ in the sums. This does not markedly change the values for the extended modes. For the noninteracting localized modes we obtain $\overline{R_{\rm gyr}}(2)=0.9$, $\overline{d}(2)=1.5$ and $\overline{R_{\rm gyr}}(4)=0.7$, $\overline{d}(4)=1.5$. Concentrating on the core of the modes the values corresponding to participation and effective mass become similar. The central atoms of the modes form low-dimensional structures which are dressed by the long-range parts of higher dimension. In average the above-defined core of a local mode comprises 12 atoms.

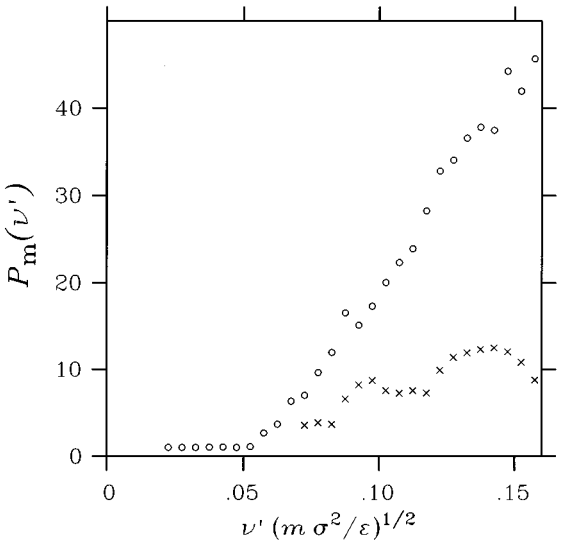

FIG. 9. Ensemble-averaged mode participation number for a soft sphere glass of $N=5488$ atoms after demixing plotted against frequency (localized modes ○, extended modes ×).

The interaction pattern of the ''pure'' local modes is very complicated and with rising frequency the number of modes which interact to form the observable modes increases rapidly. As a measure we introduce, in analogy with the participation ratio, Eq. (12), a mode participation number

$$P_M(\nu')=\left[\sum_\nu a(\nu,\nu')^4\right]^{-1}, \quad (23)$$

where the $a(\nu,\nu')$ are the expansion coefficients, Eq. (13). If a mode ν' participates equally in n modes, one has $P_M(\nu')=n$. This number is not normalized with the system size N. From Fig. 9 one sees that for $N=5488$ one has below $\nu\approx 0.05$ essentially isolated local modes (circles) with $P_M(\nu')\approx 1$. For the higher frequencies $P_M(\nu')$ increases rapidly and at $\nu=0.15$ a local mode contributes essentially to over 40 modes. The corresponding number for the extended modes is much lower. It has, however, to be kept in mind that we did not resolve the interaction between ''pure phonons'' and the $P_M(\nu')$ value therefore accounts only for the interactions with local modes.

This figure illustrates the effect of increasing the system size in the simulation. Let us consider, e.g., the modes with frequencies around $\nu=0.08$. At this frequency for the considered system with $N=5488$ we have extended modes interacting with localized modes. The mode participation number is for the local modes $P_M\approx 10$ and is mainly due to interactions between the local modes. If we would double the system size, we would not change the number of extended phonons at this frequency. They would merely extend over

the doubled volume. The concentration of localized modes would stay approximately constant; their number would double which in turn means an approximate doubling of the mode participation. The values in the figure would shift to the left and the occurrence of isolated localized modes restricted to lower ν values.

In Fig. 10 we illustrate three typical mode structures. Shown are always all atoms which have at least 20% of the maximal squared amplitude of an atom for the considered mode. The cubes are the periodicity volume. In (a) we show a mode with $\nu=0.061$, $p=0.21$, and $m_{\rm eff}=148$ which can easily be envisaged mainly as a superposition of four local modes. This is verified by the above demixing procedure. We find that four local modes contribute 80% to the squared amplitude. In (b) one of these four constituent local modes is shown, $\nu=0.062$, $p=0.028$, and $m_{\rm eff}=21$. One sees that the increase in participation ratio and effective mass caused by the mode interaction is even larger than the expected factor of 4. At higher frequencies the density of interacting modes increases strongly so that a visual decomposition is no longer possible. An example of a mainly extended mode ($\nu=0.079$, $p=0.52$, and $m_{\rm eff}=545$) is illustrated in (c). About half of its squared amplitude is given by the ideal undistorted (1,0,0) phonons. The rest is due to static scattering and interaction with local modes.

V. SOFT POTENTIAL MODEL

In the soft potential model[11,12] one describes the anomalous behavior of glasses at low temperatures in terms of soft modes which coexist with the long-wavelength phonons. The dynamics of the soft modes is described by anharmonic potentials for their dimensionless displacement $\hat{x}$,

$$\hat{V}^{\rm SP}(\hat{x})=\hat{\epsilon}^{\rm SP}[\,\hat{\eta}^{\rm SP}(\hat{x}/\sigma)^2+\hat{t}^{\rm SP}(\hat{x}/\sigma)^3+(\hat{x}/\sigma)^4]. \quad (24)$$

Here we have used the length scale σ of the potential, Eq. (1), instead of the usual scale factor a.[13] The displacement of a single atom, n, is given by $\hat{x}\sigma\mathbf{e}^n$. To follow the usual presentation we change to the displacement of a single atom, the center of the mode, by setting $\sqrt{m_{\rm eff}}x=\hat{x}$:

$$V^{\rm SP}(x)=\epsilon^{\rm SP}[\,\eta^{\rm SP}(x/\sigma)^2+t^{\rm SP}(x/\sigma)^3+(x/\sigma)^4]. \quad (25)$$

In this formulation of the model the energy scale factor $\epsilon^{\rm SP}$ is equal to the value for the potential of a single atom, $\epsilon_a^{\rm SP}$, times the number of atoms participating in the mode, N_s,

$$\epsilon^{\rm SP}=N_s\epsilon_a^{\rm SP}. \quad (26)$$

This potential can either describe a single well or a double well. In the latter case there are three equivalent sets of parameters $\eta^{\rm SP}$ and $t^{\rm SP}$. For uniqueness and to ensure an expansion around the maximum, $\eta^{\rm SP}$ has to be restricted to $\eta^{\rm SP}<\frac{9}{32}(t^{\rm SP})^2$. With this restriction $\eta^{\rm SP}>0$ implies a single-well potential and $\eta^{\rm SP}<0$ a double-well potential. One expects that the parameters $\epsilon^{\rm SP}$, $\eta^{\rm SP}$, and t will occur in a glass with probabilities $P(\epsilon_a^{\rm SP})$, $P(\eta^{\rm SP})$, and $P(t^{\rm SP})$. The soft potential model is based on the assumption that there is basically one type of soft structure, whence the $\epsilon_a^{\rm SP}$ should be given by a narrow distribution. For simplicity $\epsilon_a^{\rm SP}$ is usually taken as a constant. The values of $\eta^{\rm SP}$ and $t^{\rm SP}$ are then determined by random variations of the surroundings of the

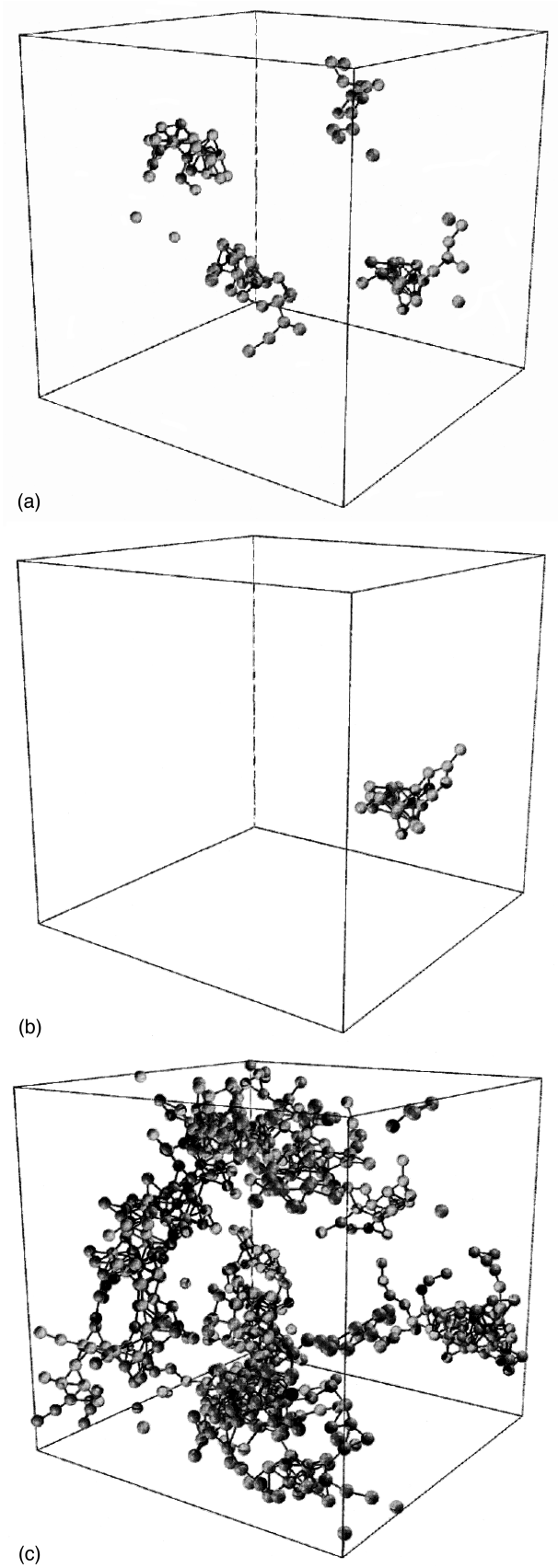

FIG. 10. Most active atoms in vibrational modes. Shown are all atoms whose squared amplitude is at least 20% of the maximal one. Bonds show nearest neighbors. The cubes depict the periodicity volume. (a) Original mode with $\nu=0.061$, $p=0.21$, and $m_{\rm eff}=148$. (b) Local mode contributing to (a) after demixing ($\nu=0.062$, $p=0.028$, and $m_{\rm eff}=21$). (c) Original mode with large phonon part ($\nu=0.079$, $p=0.52$, and $m_{\rm eff}=545$).

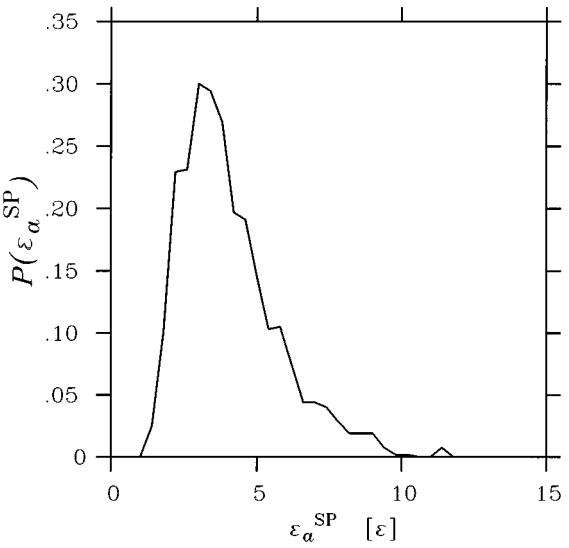

FIG. 11. Distribution function of the atomic anharmonicity ϵ_a^{SP} in the soft potential model gained from the demixed modes.

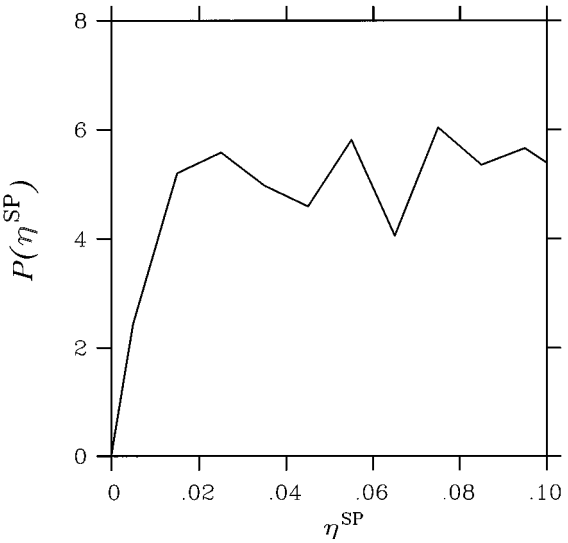

FIG. 12. Distribution function of the curvature parameter η^{SP} in the soft potential model gained from the demixed modes.

structures causing the soft modes. This implies that $P(\eta^{SP})$ and $P(t^{SP})$ are independent of each other. For low values of η^{SP} one finds $P(\eta^{SP}) \propto |\eta^{SP}|$, the so-called ''seagull'' singularity.[12] By symmetry one has $P(t^{SP}) = P(-t^{SP})$.

We have calculated for each of the local soft modes the three parameter and their distribution functions normalized to all localized modes with $\nu < 0.16$. We find for ϵ_a^{SP} an average value of 4.0 and a reasonably narrow distribution $P(\epsilon_a^{SP})$, Fig. 11, with a half width at half height of 1.5.

The corresponding averages for the vibrations of a single atom with all others at rest (Einstein vibration) are for the given potential in ideal fcc and bcc crystals of the same density 60 and 70, respectively. There one has very broad distributions of the atomic anharmonicity parameter. The soft mode values correspond to the lowest values in the bcc lattice.

The distribution $P(\eta^{SP})$, Fig. 12, shows a seagull behavior for $\eta^{SP} < 0.01$ and is nearly constant above.

The small range of ν values included in our investigation does not allow a determination of the shape of $P(\eta^{SP})$ at large η values. The end of the seagull singularity corresponds to a frequency of about $\nu = 0.05$. It has been shown that due to the seagull singularity the spectrum of local modes should be $Z_{loc} \propto \nu^4$. This is observed for in Fig. 6 for $\nu < 0.04$. The change over to $Z_{loc} \propto \nu^2$ outside the seagull singularity is washed out by statistics and the finite width of $P(\eta^{SP})$.

$P(t^{SP})$, Fig. 13, has a maximum for $t^{SP} = 0$ from where it rapidly falls off. We find no significant variation of $P(t^{SP})$ with η^{SP}. Shown are also distributions for $\eta^{SP} < 0.1$ and $\eta^{SP} > 0.1$.

The adopted quench procedure, Sec. II, ensures that configurations are always in a minimum. A fit of the soft potentials will, therefore, sometimes produce double-well potentials ($\eta^{SP} > \frac{9}{32} t^{SP}$). We find this for less than 1% of the soft modes, in seeming contradiction with the distribution of Fig. 12 which should continue to negative η^{SP}. The reason for this discrepancy between the model assumptions and our fit is inherent in the anharmonicity. In deriving the parameters of Eq. (24) we have neglected all anharmonic terms bar the one in the harmonic mode coordinate itself. In reality there is a large number of anharmonic couplings between the different modes. In simulations of defect diffusion in crystals one hardly ever finds the two minima and the saddle point lying on one line. The minimal energy path has to be described by curved coordinates. A linear extrapolation from the minimum along the soft direction in general misses the saddle point. In a glass with the much more complicated mode structure this effect would be much larger. It is, therefore, understandable why much larger numbers of double-well potentials are observed if a special algorithm is used[31] or if one extrapolates from near the saddle point.[32] We have reported earlier correlations of around 0.6 between relaxations and localized vibrations.[27]

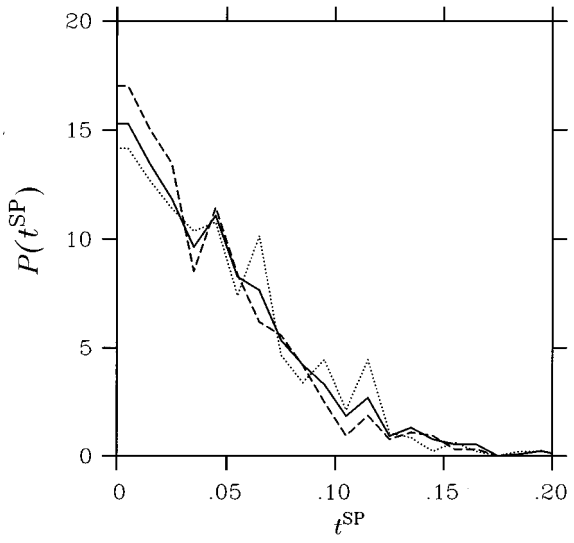

FIG. 13. Distribution function of the asymmetry parameter t^{SP} in the soft potential model gained from the demixed modes. Solid line, all local modes with $\nu < 0.16\sqrt{\epsilon/m\sigma^2}$; dashed line, only modes with $\eta < 0.1$; dotted line, only modes with $\eta > 0.1$.

VI. DISCUSSION AND CONCLUSION

Our calculations were done on a one-atom model glass. In view of the similarities between the different glasses we think them to be of general relevance for glasses.

The concentrations of localized modes and the position and strength of the boson peak will of course vary for different materials and different histories of the glass. To check the dependence of the low-frequency dynamics on glass preparation we heated our samples to 10% of the glass temperature, kept them at this temperature for a duration of about 5000 average vibration periods, and subsequently quenched them again to $T=0$. We find for the tempered glasses a volume reduction of order 10^{-3}, taken at constant external pressure. Their spectra are slightly harder due to an increase of the transverse sound velocity by about 1%. The number of soft modes with $\nu<0.16$ decreases by approximately 6%. Half of this decrease can be attributed to the general hardening of the frequencies due to the increased sound velocity. The other half indicates a reduction in the number of excess soft modes. The character of the modes, e.g., their participation ratio distribution, does not, however, change markedly. The same holds after a tempering at 15% of the glass temperature.

The reduction in the number of modes with tempering is consistent with the previous finding that the modes are centered at ''defects'' in the glass.[15,16] In tempering the most unstable of these defects will be annealed. In a one-atom glass such annihilation processes will be especially efficient, eventually leading to crystallization. It is well known that most defects cause some volume expansion. This excess volume can be used to monitor the number of defects. The volume expansion by a defect need not, however, be localized at the defect. In a crystal lattice the creation of both vacancies and interstitials causes a volume expansion of the order of one atomic volume. To create a vacancy one can imagine an atom from the bulk being placed on the surface, thus expanding the crystal by one atomic volume. After relaxation there remains localized at the vacancy a reduction in the density. In the case of an interstitial atom one imagines an atom from the surface inserted in an interstitial site. Unrelaxed one would have a volume reduction and a strong local compression at the interstitial site. The relaxation of the lattice increases the volume, even creating an excess volume, but some of the local compression remains. The excess volume is smeared out over a large region. In our case such a local compression was observed at the centers of the soft modes. This is compatible with an intersticialcy model.[44] The changed local environment will cause local internal stresses as observed earlier for another system.[17] On the other hand a description of the dynamics by scattering at density fluctuation domains seems inadequate.[45] Also an explanation in terms of coordination defects[24] is not appropriate for a close-packed metal-like glass as considered here.

Our investigation shows that the low-frequency vibrations in glasses can be understood in terms of interacting local and extended (phonon) modes. Localization has to be understood in the sense of resonant low-frequency modes.[40] This means that there is always an interaction between localized modes and phonons and in the absence of local symmetry between localized modes of similar frequencies. For low frequencies (low densities) the interaction joins the local modes into multiple-centered modes. Due to the low concentration of localized modes, the interaction between them will be weak and the dynamics becomes similar to the one in orientational glasses as discussed by Randeria and Sethna.[46] For higher frequencies when the densities of the underlying local modes and phonons are sufficiently high the resulting mixed modes can no longer be distinguished as basically localized or extended. We find that near the boson peak the mean free path of the extended phonons has decreased to their wavelength.

We have developed a method to deconvolute the exact low-frequency modes into their localized and extended parts. For the localized modes we find as in earlier investigations effective masses of ≈ 20. The cores of these modes are low dimensional, chains with side branches. The backbones are given by close-packed directions. The localized vibrations are strongly correlated with local relaxations.[26,27]

By calculating the anharmonicities of the local modes we derived the distribution functions of the parameters of the soft potential model. These are in agreement with the assumptions and results of this model. The atomic fourth-order term is reasonably well defined. It corresponds to the values found for the softest directions in the ordered structure. The distribution of the harmonic parameter η increases as predicted $\propto|\eta|$ which means an increase of the local mode spectrum $\propto\nu^4$ and of the specific heat above the tunneling regime $\propto T^5$ as observed in experiment; see Ref. 13 for references. The distribution functions of the different parameters, anharmonicity, curvature, and asymmetry, are independent. This is in agreement with the findings for two-well systems.[31]

Our results predict large mean square displacements of the atoms participating in the soft vibrations. This was recently observed in neutron scattering experiments on amorphous polymers[47] at and above the boson peak frequency, consistent with a vibrational localization to about ten monomers.

ACKNOWLEDGMENTS

We are grateful for many stimulating discussions with U. Buchenau and B.B. Laird.

*Present address: Institut für Algorithmen und Wissenschaftliches Rechnen, GMD - Forschungszentrum Informationstechnik, D-53754 Sankt Augustin, Germany.

[1] *Amorphous Solids: Low Temperature Properties*, edited by W.A. Phillips (Springer-Verlag, Berlin, 1981).

[2] *Glassy Metals I*, edited by H.-J. Günterodt and H. Beck (Springer-Verlag, Berlin, 1981).

[3] R.C. Zeller and R.O. Pohl, Phys. Rev. B **4**, 2029 (1971).

[4] P.W. Anderson, B.I. Halperin, and C.M. Varma, Philos. Mag. **25**, 1 (1972).

[5] W.A. Phillips, J. Low Temp. Phys. **7**, 351 (1972).

[6] G. Winterling, Phys. Rev. B **12**, 2432 (1975).

[7] U. Buchenau, H.M. Zhou, N. Nücker, K.S. Gilroy, and W.A. Phillips, Phys. Rev. Lett. **60**, 1318 (1988).

[8] J.-B. Suck and H. Rudin, in *Glassy Metals II*, edited by H. Beck and H.-J. Günterodt (Springer-Verlag, Berlin, 1983).

[9] K. Inoue, T. Kanaya, S. Ikeda, K. Kaji, K. Shibata, M. Misawa, and Y. Kiyaanagi, J. Chem. Phys. **95**, 5332 (1991).
[10] S. Hunklinger and M. von Schickfus in Ref. 1, p. 81.
[11] V.G. Karpov, M.I. Klinger, and F.N. Ignatiev, Sov. Phys. JETP **57**, 439 (1983).
[12] M.A. Il'in, V.G. Karpov, and D.A. Parshin, Sov. Phys. JETP **65**, 165 (1987).
[13] U. Buchenau, Yu.M. Galperin, V.L. Gurevich, and H.R. Schober, Phys. Rev. B **43**, 5039 (1991).
[14] U. Buchenau, Yu.M. Galperin, V.L. Gurevich, D.A. Parshin, M.A. Ramos, and H.R. Schober, Phys. Rev. B **46**, 2798 (1992).
[15] B.B. Laird and H.R. Schober, Phys. Rev. Lett. **66**, 636 (1991).
[16] H.R. Schober and B.B. Laird, Phys. Rev. B **44**, 6746 (1991).
[17] S.-P. Chen, T. Egami, and V. Vitek, Phys. Rev. B **37**, 2440 (1988).
[18] W. Jin, P. Vashishta, R.K. Kalia, and J.P. Rino, Phys. Rev. B **48**, 9359 (1993).
[19] C. Oligschleger and H.R. Schober, Physica A **201**, 391 (1993).
[20] J. Hafner and M. Krajčí, J. Phys. Condens. Matter **6**, 4631 (1994).
[21] P. Ballone and S. Rubini, Phys. Rev. B **51**, 14962 (1995).
[22] M. Cho, G.R. Fleming, S. Saito, I. Ohmine, and R.M. Stratt, J. Chem. Phys **100**, 6672 (1994).
[23] J. Hafner and M. Krajčí, J. Phys. Condens. Matter **5**, 2489 (1993).
[24] R. Biswas, A.M. Bouchard, W.A. Kamitakahara, G.S. Grest, and C.M. Soukoulis, Phys. Rev. Lett. **60**, 2280 (1988).
[25] F. Faupel, P.W. Hüppe, and K. Rätzke, Phys. Rev. Lett. **65**, 1219 (1990).
[26] H.R. Schober, C. Oligschleger, and B.B. Laird, J. Noncryst. Solids **156-158**, 965 (1993).
[27] C. Oligschleger and H.R. Schober, Solid State Commun. **93**, 1031 (1995).
[28] H. Miyagawa, Y. Hiwatari, B. Bernu, and J.P. Hansen, J. Chem. Phys. **88**, 3879 (1988).
[29] G. Wahnström, Phys. Rev. A **44**, 3752 (1991).
[30] J.M. Delaye and Y. Limoge, J. Phys. (France) I **3**, 2079 (1993).
[31] A. Heuer and R.J. Silbey, Phys. Rev. Lett. **70**, 3911 (1993).
[32] S.D. Bembenek and B.B. Laird, Phys. Rev. Lett. **74**, 936 (1995).
[33] R. Cotteril and J. Madsen, Phys. Rev. B **33**, 262 (1986).
[34] W.G. Hoover, S.G. Gray, and K.W. Johnson, J. Chem. Phys. **55**, 1129 (1971).
[35] U. Bengtzelius, W. Götze, and A. Sjölander, J. Phys. C **17**, 5915 (1984).
[36] W.G. Hoover, D.A. Young, and R. Grover, J. Chem. Phys. **56**, 2207 (1972).
[37] W.C. Swope, H.C. Andersen, P.H. Berens, and K.R. Wilson, J. Chem. Phys. **76**, 637 (1982).
[38] R. Fletcher and C.M. Reeves, Comput. J. **7**, 149 (1964).
[39] Harwell Subroutine Library, AERE Harwell, Didcot, UK.
[40] A.A. Maradudin, E.W. Montroll, G.H. Weiss, and I.P. Ipatova, *Theory of Lattice Dynamics in the Harmonic Approximation*, Solid State Physics Suppl. 3 (Academic, New York, 1971).
[41] H.R. Schober, V.K. Tewary, and P.H. Dederichs, Z. Phys. B **21**, 255 (1975).
[42] V.L. Gurevich, D.A. Parshin, J. Pelous, and H.R. Schober, Phys. Rev. B **48**, 16318 (1993).
[43] F. Yonezawa, J. Non-Cryst. Solids **35/36**, 29 (1980).
[44] A.V. Granato, Phys. Rev. Lett. **68**, 974 (1992).
[45] S.R. Elliott, Europhys. Lett. **19**, 201 (1992).
[46] M. Randeria and J.S. Sethna, Phys. Rev. B **38**, 12607 (1988); **41**, 7784 (1990).
[47] U. Buchenau, C. Pecharromán, and B. Frick (private communication).